

Global relativistic effects in chaotic scatteringJuan D. Bernal,^{1,*} Jesús M. Seoane,¹ and Miguel A. F. Sanjuán^{1,2}¹*Nonlinear Dynamics, Chaos and Complex Systems Group, Departamento de Física, Universidad Rey Juan Carlos, Tulipán s/n, 28933 Móstoles, Madrid, Spain*²*Institute for Physical Science and Technology, University of Maryland, College Park, Maryland 20742, USA*

(Received 24 November 2016; published 8 March 2017)

The phenomenon of chaotic scattering is very relevant in different fields of science and engineering. It has been mainly studied in the context of Newtonian mechanics, where the velocities of the particles are low in comparison with the speed of light. Here, we analyze global properties such as the escape time distribution and the decay law of the Hénon-Heiles system in the context of special relativity. Our results show that the average escape time decreases with increasing values of the relativistic factor β . As a matter of fact, we have found a crossover point for which the KAM islands in the phase space are destroyed when $\beta \simeq 0.4$. On the other hand, the study of the survival probability of particles in the scattering region shows an algebraic decay for values of $\beta \leq 0.4$, and this law becomes exponential for $\beta > 0.4$. Surprisingly, a scaling law between the exponent of the decay law and the β factor is uncovered where a quadratic fitting between them is found. The results of our numerical simulations agree faithfully with our qualitative arguments. We expect this work to be useful for a better understanding of both chaotic and relativistic systems.

DOI: [10.1103/PhysRevE.95.032205](https://doi.org/10.1103/PhysRevE.95.032205)**I. INTRODUCTION**

Chaotic scattering in open Hamiltonian systems has been a broad area of study in nonlinear dynamics, with applications in numerous fields in physics (see Refs. [1] and [2]). This topic is essentially defined by a *scattering region* where there are interactions between incident particles and a potential. Outside this region the influence of the potential on the particles is negligible and the motions of the incident particles are uniform. For many applications of physical interest, the equations of motion of the test particles are nonlinear and the resultant dynamics is chaotic in the scattering region. Therefore, slightly similar initial conditions may describe completely different trajectories. Since the system is open, this region possesses exits through which the particles may enter or escape. Quite often, particles starting in the scattering region bounce back and forth for a finite time before escaping. In this sense, chaotic scattering could be presented as a physical manifestation of transient chaos [3,4].

Using the Newtonian approximation for modeling the dynamics of the system is the most widely accepted convention in physics and engineering applications when the speed of objects is low compared to the speed of light [5]. Nevertheless, if the dynamics of the system is really sensitive to the initial conditions, the trajectories predicted by the Newtonian scheme rapidly disagree with the ones described by the special relativity theory (see Refs. [6–9]). Recently, there have been some results [10] pointing out that the global properties of the dynamical systems, such as the dimension of the nonattracting chaotic invariant set, are more robust and the Newtonian approximation actually provides accurate enough results for them in slow chaotic scattering motion. The goal of this paper is to show that there are relevant global properties of chaotic scattering systems that indeed do depend on the effect of the Lorentz transformations and we may consider the special

relativity scheme when we want to describe them in a realistic manner, even for low velocities. Specifically, we focus our study on both the average escape times and the decay law of the particles from the scattering region, which are quite important global properties in scattering systems. The authors of the present work have shown the effect of external perturbations such as noise and dissipation in some Hamiltonian systems (see Refs. [1] and [11]). However, the consideration of the relativistic framework to the system dynamics cannot be considered an external perturbation like the noise or dissipation, although the global properties of the system also change.

Henceforth, we refer to any effect where the Lorentz transformations have been considered as relativistic. Likewise, we say that any property or object is nonrelativistic or Newtonian when we take into consideration not the Lorentz transformations but the Galilean ones.

This paper is organized as follows. In Sec. II, we describe our prototype model, the relativistic Hénon-Heiles system. The effects of the Lorentz transformation on the average escape time of the particles and their decay law are reported in Secs. III and IV. In Sec. V, we give a heuristic reasoning based on energetic considerations to explain the results obtained in previous sections. In Sec. VI, we characterize the decay law of relativistic particles. A discussion and the main conclusions of this paper are presented in Sec. VII.

II. MODEL DESCRIPTION

We focus our attention here on the global effects of relativistic corrections in a paradigmatic chaotic scattering system, such as the Hénon-Heiles Hamiltonian. The two-dimensional potential of the Hénon-Heiles system is defined by

$$V(x, y) = \frac{1}{2}k(x^2 + y^2) + \lambda \left(x^2 y - \frac{1}{3}y^3 \right). \quad (1)$$

In 1964 Hénon and Heiles proposed considering this potential in the proper system of units where $k = \lambda = 1$ (see

*juandiego.bernal@urjc.es

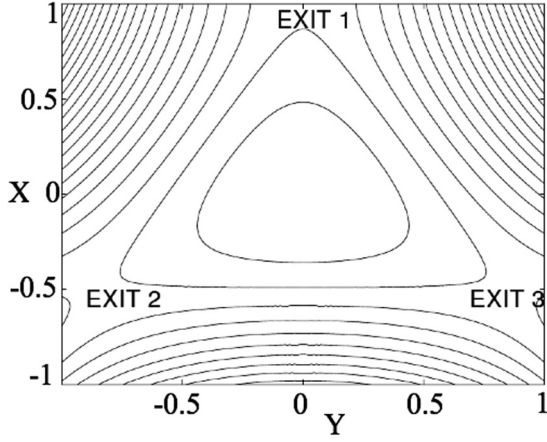


FIG. 1. Isopotential curves for the Hénon-Heiles potential: they are closed for energies below the nonrelativistic threshold energy escape $E_e = 1/6$. Three exits for energy values above $E_e = 1/6$ are shown.

Ref. [12]). Its isopotential curves are shown in Fig. 1. Due to the triangular symmetry of the system, the exits are separated by an angle of $2\pi/3$ radians. For the sake of clarity, we call the upper exit ($y \rightarrow +\infty$) exit 1, the left one ($y \rightarrow -\infty, x \rightarrow -\infty$) exit 2, and the right exit ($y \rightarrow -\infty, x \rightarrow +\infty$) exit 3.

We define the nonrelativistic total mechanical energy and we call it the Newtonian energy, E_N ; $E_N = T(\mathbf{p}) + V(\mathbf{r})$, where T is the kinetic energy of the particle, $T = \mathbf{p}^2/2m$, \mathbf{p} is its linear momentum, $V(\mathbf{r})$ is the potential energy, and \mathbf{r} is its vector position. Depending on the value of the Newtonian energy, the trajectory of any incident particle is trapped in the scattering region ($E_N \in [0, 1/6]$) or eventually escapes from it up to ∞ for $E_N > 1/6$. Actually there are three regimes of motion, depending on the initial value of the energy: (a) closed nonhyperbolic, $E_N \in [0, 1/6]$; (b) open nonhyperbolic, $E_N \in (1/6, 2/9)$; and (c) open hyperbolic, $E_N \in [2/9, +\infty)$ [13]. Within the first energy range, all the trajectories are trapped and there is no exit by which any particle may escape. There is a wide variety of possible motions in this energy range, from periodic and quasiperiodic trajectories to chaotic trajectories. However, in the range of $E_N \in (1/6, 2/9)$ the regime is open nonhyperbolic, the energy is high enough to allow escapes from the scattering region, and KAM tori coexist with chaotic saddles, which typically results in an algebraic decay in the survival probability of a particle in the scattering region. On the contrary, if $E_N \in [2/9, +\infty)$, the regime is open hyperbolic and all the periodic trajectories are unstable, therefore there is no KAM tori in the phase space.

If we consider the motion of a relativistic particle moving in an external potential energy $V(\mathbf{r})$, the Hamiltonian (i.e., the total energy) is

$$H = E = mc^2 + V(\mathbf{r}) = \sqrt{m^2c^4 + c^2\mathbf{p}^2} + V(\mathbf{r}), \quad (2)$$

where m is the particle's rest mass and c is the speed of light. Then the Hamilton's canonical equations are

$$\begin{aligned} \dot{\mathbf{p}} &= -\frac{\partial H}{\partial \mathbf{r}} = -\nabla V(\mathbf{r}), \\ \dot{\mathbf{r}} = \mathbf{v} &= \frac{\partial H}{\partial \mathbf{p}} = \frac{\mathbf{p}}{m\gamma}, \end{aligned} \quad (3)$$

where the Lorentz factor γ is defined as

$$\gamma = \sqrt{1 + \frac{\mathbf{p}^2}{m^2c^2}} = \frac{1}{\sqrt{1 - \frac{v^2}{c^2}}}. \quad (4)$$

When $\gamma = 1$ the Newtonian equations of motion are recovered from Eq. (3). That is the reason why the usual convention is to consider the Newtonian scheme a good approximation for slow motion, where $\gamma \approx 1$. We define β as the ratio v/c , where v is the modulus of the vector velocity \mathbf{v} . Then the Lorentz factor can be rewritten as $\gamma = \frac{1}{\sqrt{1-\beta^2}}$. Whereas $\gamma \in [1, +\infty)$, the range of values for β is $[0, 1]$. However, γ and β express essentially the same thing: how high the velocity of the object is compared to the speed of light. Henceforth, we use β instead of γ to show our results, for convenience.

Taking into consideration Eqs. (1) and (3), the relativistic equations of motion of a scattering particle of unit rest mass ($m = 1$) interacting with the Hénon-Heiles potential are

$$\begin{aligned} \dot{x} &= \frac{p}{\gamma}, \\ \dot{y} &= \frac{q}{\gamma}, \\ \dot{p} &= -x - 2xy, \\ \dot{q} &= -y - x^2 + y^2, \end{aligned} \quad (5)$$

where p and q are the two components of the linear momentum \mathbf{p} .

In the present work, we aim to isolate the effects of variation of the Lorentz factor γ (or β as previously shown) from the rest of the variables of the system such as, for instance, the initial velocity of the particles and its energy. For this reason, we use different systems of units so that γ is the only parameter in the equations of motion [Eq. (5)] that may vary. Therefore, we analyze the evolution of the properties of the system when β varies, comparing these properties with the characteristics of the nonrelativistic system. For this comparison, during our numerical computations we choose the same value of the initial velocity, $v = 0.583$, in different systems of units, corresponding to a Newtonian energy $E_N = 0.17$, that is, the open nonhyperbolic regime, as described in Sec. II. In this regime the Hénon-Heiles system exhibits the richest variety of behaviors. As an example for the sake of clarity, we consider an incident particle coming from ∞ to the scattering region. Imagine that we measure the properties of the incident particle in the Planck system of units. In this system, the speed of light is $c = 1c$, that is, the variable speed is measured as a multiple of the speed of light c instead of in m/s, for instance. Likewise, in the Planck units, the mass is expressed as a multiple of the Planck mass m_P (which is $m_P \approx 2.2 \times 10^{-8}$ kg). According to our measures, the resting mass of the particle is the unit $m = 1m_P$. Likewise, we measure its inner speed as $v = 0.583c$. According to the Newtonian scheme, the classical energy of the particle is $E_N = \frac{1}{2}v^2 \approx 0.17E_P$, where E_P is the Planck energy, the unit for the energy in the Planck system ($E_P \approx 1.96 \times 10^9$ J). Now we consider another incident particle with a different resting mass and velocity, however, we choose the International System of Units (SI) to

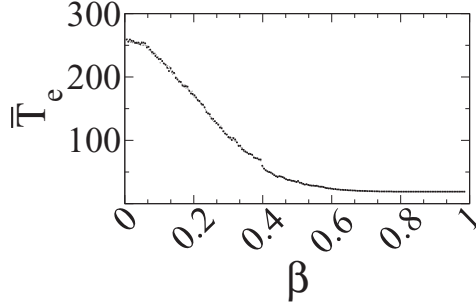


FIG. 2. Average escape time \bar{T}_e of 10 000 particles inside the scattering region with initial velocity $v = 0.583$. Initial conditions are $(x_0, y_0, \dot{x}_0, \dot{y}_0) = (0, 0, v \cos(\varphi), v \sin(\varphi))$, with shooting angle $\varphi \in [0, 2\pi]$. We use 500 values of β in our calculations. There is a linear decrease in \bar{T}_e up to $\beta \approx 0.4$. Indeed at $\beta \approx 0.4$ there is a leap where the linearly decreasing trend of \bar{T}_e changes abruptly.

measure its properties. In this case, we obtain that its resting mass is again the unit, although now the rest mass is 1 kg, $m = 1$ kg, and its velocity is $v = 0.583$ m/s. The speed of light in SI is $c \approx 3 \times 10^8$ m/s. The initial Newtonian energy of the particle is $E_N \approx 0.17$ J in SI, but now the initial velocity is almost negligible compared to the speed of light, that is, $\beta = v/c = 0.583/3 \times 10^8 \approx 2 \times 10^{-9}$. Therefore, from the perspective of the equations of motion of both particles, when we consider just the Galilean transformations, we can conclude that the behavior of the particles will be the same since $V(x, y)$ of Eq. (1) is equal in both cases, as long as the parameters $k = \lambda = 1$ in their respective system of units. However, they are completely different when relativistic corrections are considered because the Lorentz factor γ affects the equations of motion by the variation of β , regardless of the selected system of units. To summarize, the objective of our numerical computations and analysis is to study the effect of γ on the equations of motion, so the key point is to set the speed of light c as the threshold value of the speed of particles, regardless of the system of units we are considering.

III. NUMERICAL RESULTS ON THE ESCAPE TIME

In this section we study the discrepancies between the relativistic and the nonrelativistic corrections when we analyze the *average escape time*, \bar{T}_e , of the system, which is an essential global property in chaotic scattering problems. The *escape time*, T_e , of an incident particle is defined as the time it spends in the scattering region. For times above T_e , the particle travels to ∞ after having crossed one of the three exit boundaries, which are extremely unstable trajectories called *Lyapunov orbits* (see Ref. [14]). In the case of the Hénon-Heiles system, the Lyapunov trajectories exist for energies higher than $E_e = 1/6$. The higher the energy, the shorter the escape times. When we consider a large number of particles and we average their individual T_e values, then we obtain the global property \bar{T}_e , which is a unique and characteristic property of the system. We represent in Fig. 2 the average escape time, \bar{T}_e , of 10 000 particles shot inside the scattering region with an initial velocity $v = 0.583$. The initial conditions are $(x_0, y_0, \dot{x}_0, \dot{y}_0) = (0, 0, v \cos(\varphi), v \sin(\varphi))$,

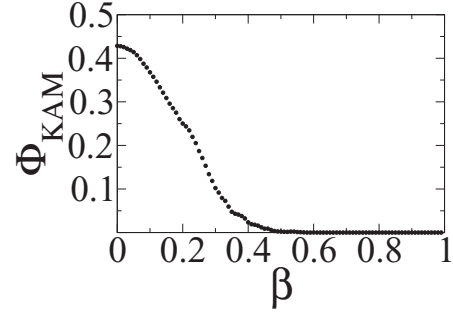


FIG. 3. Percentage of trapped particles in the scattering region: Φ_{KAM} , expressed as a decimal, at t_{max} , is directly proportional to the Lebesgue measure of the KAM islands on the Poincaré surface of the section. At $\beta \approx 0.4$ there are just a few particles trapped in the scattering region.

with shooting angle $\varphi \in [0, 2\pi]$. We use 500 values of β for our calculations. The Newtonian average escape time in Fig. 2 is the first point in the graph, when $\beta \rightarrow 0$. This value is indeed the inner average escape time of the particles. As a reminder, this is the time as seen by an observer who is stationary with regard to the reference frame of the particle. Then, if we average the measures of the inner escape time of the 10 000 particles, we get the value of \bar{T}_e when $\beta \rightarrow 0$. As shown in Fig. 2, there is a clear influence of the Lorentz factor variation on the average escape time \bar{T}_e . It is noteworthy that, in the most general sense, we define scattering as the problem of obtaining the relationship between an *input* variable taken from outside the scattering region and an *output* variable, which characterizes the final state of the system after interacting with the scattering region (see Ref. [2]). However, starting the numerical experiments within the scattering region is a convention frequently used in the scientific literature (see, for example, Refs. [13] and [15], [16], and [17]). The reason behind this is to take advantage of the well-known topological structure of the escape basins resulting from the Poincaré surface of section (\dot{y}, y) for $x(0) = 0$. Therefore it is implicitly assumed that the initial conditions chosen for the computations may correspond to trajectories which come from outside the scattering region, and after bouncing back and forth for a certain time in the scattering region, they pass through $x = 0$ at a certain velocity (\dot{x}, \dot{y}) . This is the precise instant when the simulations start and the initial conditions are set as $(x = 0, y, \dot{x}, \dot{y})$. According to Fig. 2, there is a relevant decrease in \bar{T}_e up to $\beta \approx 0.4$. Indeed at $\beta \approx 0.4$ there is a leap where the linearly decreasing trend of \bar{T}_e changes abruptly. This can be explained when we highlight that at $\beta \approx 0.4$ the KAM islands are almost destroyed and there are just a few trajectories trapped in the scattering region forever. In fact, as shown in the literature (see Ref. [18]), KAM islands exhibit a certain stickiness in the sense that their presence in the phase space provokes longer transients inside the scattering region. In order to confirm the destruction of the KAM island at $\beta \approx 0.4$, we analyze in Fig. 3 the percentage, expressed as a decimal, of particles trapped in the scattering region at t_{max} . We call this percentage ϕ_{KAM} and it is directly related to the presence of KAM islands and its Lebesgue measure in the Poincaré surface of the section.

To calculate Φ_{KAM} we have again considered 10 000 particles inside the scattering region with initial conditions $(x_0, y_0, \dot{x}_0, \dot{y}_0) = (0, 0, 0.583 \cos(\varphi), 0.583 \sin(\varphi))$ and shooting angle $\varphi \in [0, 2\pi]$. Then we compare the number of particles remaining in the scattering region after a long transient, t_{max} , with the total number of initially shot particles, obtaining the quantity Φ_{KAM} for a certain value of β . Finally, we take different values of β and we represent Φ_{KAM} vs β to get Fig. 3. The results point out that, even for low velocities ($\beta < 0.2$), the number of trapped particles decreases as β increases. When $\beta \approx 0.4$ there are almost no particles trapped in the scattering region, which is a direct proof of the destruction of the KAM islands. It is noteworthy that the shapes of both curves, $\bar{T}_e(\beta)$ and $\Phi_{\text{KAM}}(\beta)$, as shown in Figs. 2 and 3, are very similar, which expresses the influence of the KAM destruction mechanism over the global properties of the system.

In Sec. V we discuss the reasons behind the trend of the average escape time \bar{T}_e of the system under the variation of β in Fig. 2.

IV. NUMERICAL RESULTS ON THE DECAY LAW

In this section, we report the numerical results that we have obtained from the analysis of another fundamental piece of any chaotic scattering system, the time delay statistics $P(t)$ of the system (see Ref. [1]), when we consider the Lorentz corrections. Suppose that we pick many different initial conditions at random in some interval of the domain. Then we examine the resulting trajectory for each value and determine the time t that its trajectory spends in the scattering region. The fraction of trajectories with a *time delay* between t and $t + dt$ is $P(t)dt$. For open nonhyperbolic dynamics with bounding KAM surfaces in the scattering region, one finds that for large t the time delay statistics, $P(t)$, decays algebraically as follows:

$$P(t) \sim t^{-\alpha}. \quad (6)$$

An algebraic decay law like that described in Eq. (6) is also found in higher dimensional Hamiltonian systems when the phase space is partially filled with a KAM torus (see Ref. [19]).

For our simulations we have considered 10 000 particles shot into the scattering region at initial velocities $v \approx 0.5831$. The initial conditions are $(x_0, y_0, \dot{x}_0, \dot{y}_0) = (0, 0, v \cos(\varphi), v \sin(\varphi))$, with shooting angle $\varphi \in [0, 2\pi]$. Then we get the fraction of particles within the scattering region between t and $t + dt$, that is, $P(t)dt$, and we represent $\log_{10}(P(t))$ vs $\log_{10}(t)$ to get the value of the parameter α (the slope of the resulting straight line). Calculating α for different values of β , we obtain the evolution of the parameter α with β . In Fig. 4 we can see that the numerical values of $\alpha(\beta)$ fit a quadratic curve as $\alpha \approx A_0 + A_1\beta + A_2\beta^2$, with $A_0 = 0.46138$, $A_1 = -2.5311$, and $A_2 = 15.185$. We have indeed found that the decay law of the time delay statistics is algebraic, according to Eq. (6), for the range of energies where the regime of the system is open nonhyperbolic. For the initial conditions chosen to perform our computations, this regime takes up to $\beta \approx 0.4$. The values of the coefficients A_0 , A_1 , and A_2 are exclusively valid in the range of values that we have considered for the nonlinear fitting, $[0.05, 0.4]$. However, we can expect that the value of the parameter α in the

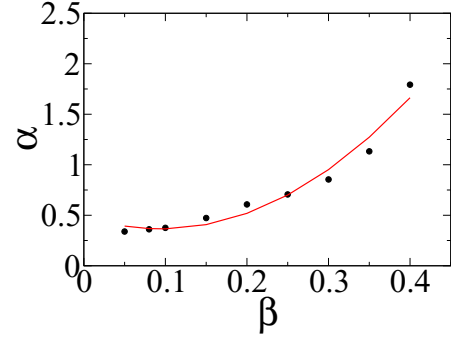


FIG. 4. Evolution of the parameter α : the exponent α of the algebraic decay law [see Eq. (6)] in the relativistic Hénon-Heiles system under the variation of β . The initial velocity of $v \approx 0.5831$. There is a quadratic trend, $\alpha \approx A_0 + A_1\beta + A_2\beta^2$, where $A_0 = 0.46138$, $A_1 = -2.5311$, and $A_2 = 15.185$.

nonrelativistic framework may be similar to the one obtained by the quadratic formula. This is because the minimum value of the range considered for the fitting, that is, 0.05, is relatively close to $\beta \rightarrow 0$. Indeed, the coefficient $A_0 = 0.461$ may be deemed a good approximation of the Newtonian framework since this yields a value of α equal to 0.386.

As the speed of particles increases and $\beta > 0.4$, the measure of bounding KAM surfaces is practically negligible in the scattering region and all the trajectories exit from there. The decay law of the particles becomes exponential according to Eq. (7),

$$P(t) \sim e^{-t/\tau}, \quad (7)$$

where $1/\tau$ is the characteristic time for the scatterer.

We can proceed similarly to calculate the evolution of the parameter τ while β is increased. We shoot 10 000 particles into the scattering region with initial conditions $(x_0, y_0, \dot{x}_0, \dot{y}_0) = (0, 0, v \cos(\varphi), v \sin(\varphi))$, with $v \approx 0.5831$ and shooting angle $\varphi \in [0, 2\pi]$. Getting the fraction of particles into the scattering region between t and $t + dt$, we represent $\ln(P(t))$ vs t . The slope of the resulting straight line is the value of the parameter τ . If we do the same for increasing values of β , we obtain the relation between τ and β . Figure 5 shows the quadratic evolution of the numerical data on the

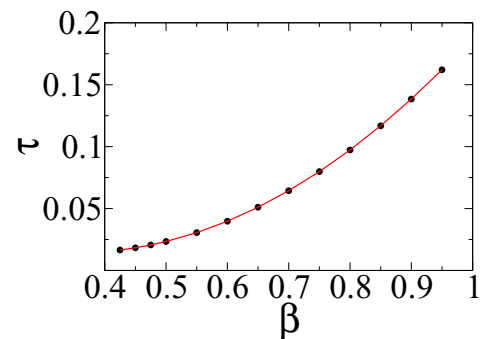


FIG. 5. Evolution of the parameter τ of the exponential decay law of the relativistic Hénon-Heiles system under the variation of β . The initial velocity of $v \approx 0.5831$. The trend is quadratic, $\tau \approx \tau_0 + \tau_1\beta + \tau_2\beta^2$, where $\tau_0 = 0.065207$, $\tau_1 = -0.028988$, and $\tau_2 = 0.4125$.

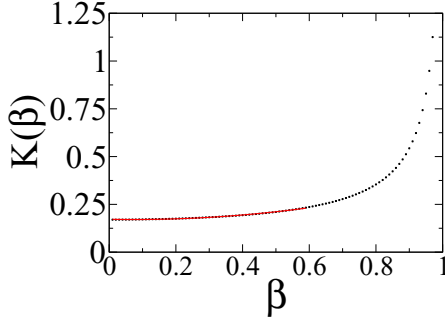


FIG. 6. Representation of the relativistic kinetic energy of the system as an explicit function of β , $K(\beta)$ [see Eq. (8)]. While the system is in the open nonhyperbolic regime, the kinetic energy fits a quadratic curve. $K(\beta) \approx K_0 + K_1\beta + K_2\beta^2$, where $K_0 = 0.25676$, $K_1 = -0.77133$, and $K_2 = 1.2553$.

parameter τ , while the Lorentz factor varies according to $\tau \approx \tau_0 + \tau_1\beta + \tau_2\beta^2$, where $\tau_0 = 0.065207$, $\tau_1 = -0.028988$, and $\tau_2 = 0.4125$.

In the next section we see why the numerical values of $\alpha(\beta)$ and $\tau(\beta)$ follow a quadratic trend.

V. DISCUSSION OF THE ESCAPE TIME AND THE DECAY LAW

In the present section we follow a qualitative approach to discuss the trends of the global properties of the system that we have studied in Secs. III and IV as $\bar{T}_e(\beta)$, $\alpha(\beta)$, and $\tau(\beta)$. First, we take the relativistic kinetic energy of the system, $K = m\gamma c^2 - mc^2$, as an explicit function of β :

$$K(\beta) = \frac{v^2}{\beta^2\sqrt{1-\beta^2}} - \frac{v^2}{\beta^2}. \quad (8)$$

In Fig. 6 we represent $K(\beta)$. If we try to fit the curve $K(\beta)$ to a polynomial while the system is in the open nonhyperbolic regime (up to $\beta \approx 0.4$), we see that the numerical values of the relativistic kinetic energy of the system fit a quadratic curve: $K(\beta) \approx K_0 + K_1\beta + K_2\beta^2$, where $K_0 = 0.25676$, $K_1 = -0.77133$, and $K_2 = 1.2553$.

The parameter α in Eq. (6) is related to the square of the average speed at which the particles leave the scattering region. The higher the α , the faster $P(t)$ decays and, therefore, the faster the particles exit from the scattering region. Therefore, we may consider that the parameter α should be directly proportional to the energy of the system, in a linear way. This is indeed the case for the nonrelativistic Hénon-Heiles system. In Fig. 7 we show the linear relation between the parameter α and the total energy of the classical Hénon-Heiles system, E_N , in the open nonhyperbolic regime. This numerical result was also demonstrated in previous works [20]. Then, if the energy of the system fits a quadratic curve of β and it is also directly proportional to α , we may expect that the parameter α will show a quadratic trend when β is varied.

As we did for the open nonhyperbolic regime, now we can proceed to fit the curve $K = K(\beta)$ to a quadratic curve, while the system is in the open hyperbolic regime, $\beta \in (0.4, 0.8]$. This is shown in Fig. 7. It yields a second-order curve, $K(\beta) \approx K_0 + K_1\beta + K_2\beta^2$, where $K_0 = 0.254$, $K_1 =$

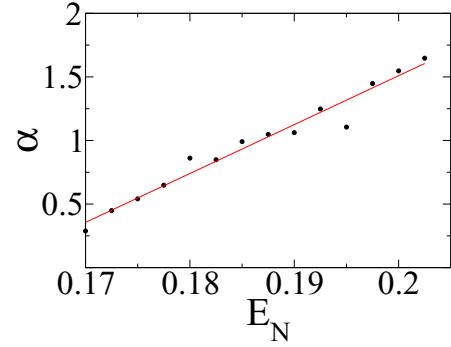


FIG. 7. Linear correlation between α and the total energy of the nonrelativistic Hénon-Heiles system.

-0.3869 , and $K_2 = 5968$. $R^2 = 0.9971$. The goodness of the fit to a quadratic curve of the numerical data on $K = K(\beta)$ in the open hyperbolic regime is quite high so we can conclude that, within this energy regime, $K \propto \beta^2$. The parameter τ in Eq. (7) is also related to the square of the average speed at which the particles leave the scattering region. Then we can again conclude that τ is linearly proportional to the energy of the system, and therefore, this explains why the numerical values of $\tau(\beta)$ follow a quadratic trend for the considered range of β .

We are now in a position to understand the linear trend of the curve $\bar{T}_e(\beta)$ before the KAM island destruction at $\beta \approx 0.4$ as shown in Fig. 2. If $K \propto \alpha$ and $\alpha \propto \beta^2$, considering that β is a magnitude related to the velocity of the particles, and this is inversely proportional to the escape time, then $1/\bar{T}_e \propto \beta^2$. In Fig. 8, we can see the results obtained from our computations. The relation between $1/\bar{T}_e$ and β^2 is linear. The interesting result is that a transition from $\beta \in [0, 0.4)$ (or $\beta^2 \in [0, 0.16)$ in the graph) to $\beta \in [0.4, 0.6)$ (or $\beta^2 \in [0.16, 0.40)$) was detected. This transition corresponds to the destruction of the KAM tori (about $\beta \sim 0.4$). This explains the leap shown in Fig. 2 at $\beta \sim 0.4$. This is also the value at which the percentage of trapped particles turns sharply towards 0 in Fig. 3. Both slopes of the straight lines in Fig. 8 determine the speed of particles

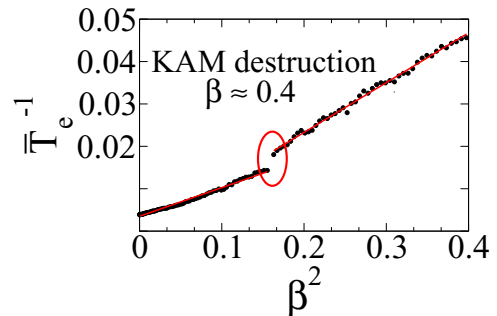


FIG. 8. Analysis of the relation between the average escape times of particles \bar{T}_e and β : the linear relation between $1/\bar{T}_e$ and β^2 . At $\beta \sim 0.4$ (that is, $\beta^2 \sim 0.16$ in the graph), we can see a transition corresponding to the destruction of the KAM tori. This explains the leap that is shown in Fig. 2 at $\beta \sim 0.4$ and why the percentage of trapped particles in the scattering region turns sharply towards 0 in Fig. 3.

exiting the scattering region. This is more numerical evidence of the KAM island stickiness.

Likewise, since $\tau \propto \beta^2$ according to Fig. 5 and we can again state that β is inversely proportional to the escape time, $1/\bar{T}_e \propto \beta^2$. Therefore, the same reasoning can be used to explain the behavior in Fig. 2 from $\beta \sim 0.4$ onward.

VI. DECAY-LAW CHARACTERIZATION

In previous studies (see Ref. [20]), Zhao and Du derived a formula for the exponential decay law, setting the parameter τ in Eq. (7) as a function of the energy of the nonrelativistic Hénon-Heiles system (see Ref. [20]). The regime of energies considered by them was the open hyperbolic one, with the model simplified by the assumption of the nonexistence of KAM islands for Newtonian energies higher than $E_N = 1/6$. In this section we apply a similar methodology for the open hyperbolic regime but considering the relativistic corrections in order to find a theoretical expression for the escape rate of the Hénon-Heiles system. The phase-space distribution can generally be expressed as

$$\psi(p, q) = \frac{\delta(\Delta E - H(p, q))}{\int dp dq \delta(\Delta E - H(p, q))}, \quad (9)$$

where p and q are the coordinates of the linear momentum (see Ref. [21]). δ is the operator that expresses a small variation of the variables in parentheses. ΔE is the difference between the relativistic mechanical energy, $K + V = E - mc^2$, and the threshold energy where the whole phase space of the system is chaotic and the particles may escape from the scattering region, $E_e = 1/6$. For convenience and simplicity, we have selected $K + V$ instead of the total relativistic energy E in the following calculations. In fact, the constant value of ΔE equals the kinetic energy of the particle when it is moving freely outside the scattering region according to Eq. (8). When it is under the effect of the Hénon-Heiles potential V , then the kinetic and the potential energy are continually being exchanged in order to keep the sum $K + V$ constant. ΔE is a conserved quantity and the following reasoning is completely valid. As described by Zhao and Du in Ref. [20], the phase-space distribution can be rewritten in terms of (x, y, θ)

as $\rho(x, y, \theta) = \frac{1}{2\pi S(\Delta E)}$, where θ is the angle between the direction of the momentum \mathbf{p} and the y axis. $S(\Delta E)$ is the area of the well. To define the area of the well, we have to consider the straight lines which contain the three saddle points of the Hénon-Heiles system and are perpendicular to the direction of the bisector lines of the equilateral triangle arranged by these three saddle points. Therefore, S is the region bounded by the well contour lines and the aforesaid straight lines. Given N particles in the S region, the number of particles leaving the well through the opening at a saddle point [for instance, $P_1 = (0, 1)$] in a unit time can be expressed as $N \int_{x_A}^{x_B} dx \int_{-\pi/2}^{\pi/2} \rho(x, y, \theta) v(x, y) \cos(\theta) d\theta$, where the integral in x is along the straight line which contains P_1 . The limits of integration x_A and x_B are the points where the contour lines of the Hénon-Heiles potential intersect the straight line that contains P_1 . If we note the triangular symmetry of the system, the number of particles leaving the well from the three openings in a unit time is just three times the previous result.

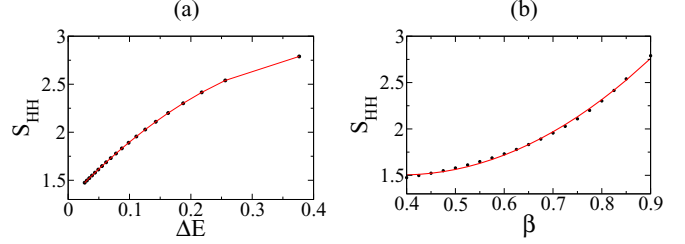


FIG. 9. Area of well S of the Hénon-Heiles system. (a) Evolution of S under the variation of energy of the system ΔE . The initial velocity is $v \approx 0.5831$. The trend is quadratic, $S(\Delta E) = S_0 + S_1 \Delta E + S_2 \Delta E^2$, with $S_0 = 1.299$, $S_1 = 6.7271$, and $S_2 = -7.3541$. The regime of considered energies is the hyperbolic one, from $\beta = 0.4$ on. The maximum value of the energy ΔE corresponds to $\beta = 0.9$. (b) Area of well S as a function of β . The trend is quadratic, $S(\beta) = s_0 + s_1 \beta + s_2 \beta^2$, with $s_0 = 2.2321$, $s_1 = -3.7433$, and $s_2 = 4.8112$.

The change of N with respect to t is

$$\begin{aligned} \frac{dN(t)}{dt} &= -3N(t)\rho \int_{-\pi/2}^{\pi/2} \cos(\theta) d\theta \int_{-\sqrt{2\Delta E/3}}^{\sqrt{2\Delta E/3}} \\ &\times \sqrt{2(\Delta E - 3x^2/2)} dx = -2\pi\sqrt{3}\Delta E\rho N(t). \end{aligned} \quad (10)$$

If we compare this result with Eq. (7), we obtain the analytical expression for the escape rate as

$$\tau(\Delta E) = \frac{\sqrt{3}\Delta E}{S(\Delta E)}. \quad (11)$$

There is no algebraic approach to obtain the expression for $S = S(\Delta E)$, but we can determine it by applying an indirect method such as, for instance, the Monte Carlo method. In Fig. 9(a) we represent the area of the well S as a function of ΔE . The numerical results fit a quadratic polynomial: $S(\Delta E) = S_0 + S_1 \Delta E + S_2 \Delta E^2$, with $S_0 = 1.299$, $S_1 = 6.7271$, and $S_2 = -7.3541$. The value of S_0 is in fact the area of the equilateral triangle whose vertexes are the three saddle points of the Hénon-Heiles system, that is, $S_0 = \frac{3\sqrt{3}}{4}$. Therefore, we can obtain the expression of $\tau = \tau(\Delta E)$ as

$$\tau(\Delta E) = \frac{\sqrt{3}\Delta E}{S_0 + S_1 \Delta E + S_2 \Delta E^2}. \quad (12)$$

In Fig. 9(b) we show S as a function of β . Again, the numerical results fit a quadratic relation: $s(\beta) = s_0 + s_1 \beta + s_2 \beta^2$, with $s_0 = 2.2321$, $s_1 = -3.7433$, and $s_2 = 4.8112$.

We can obtain the analytic expression of $\tau = \tau(\beta)$ from Eq. (12) because the conserved value of ΔE must agree with Eq. (8) when it is applied to a free-moving particle. Then we express $\tau(\beta)$ as

$$\tau(\beta) = \sqrt{3} \frac{(K_0 + K_1 \beta + K_2 \beta^2) - E_e}{s_0 + s_1 \beta + s_2 \beta^2}, \quad (13)$$

where we have expressed the value of the conserved energy of the system ΔE as $K_0 + K_1 \beta + K_2 \beta^2 - E_e$. Since Eq. (13) is a fraction of two quadratic polynomials, it can be expressed as

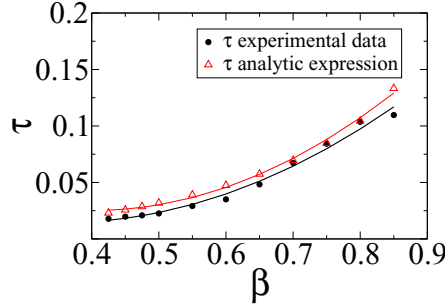


FIG. 10. Comparison between the data for the parameter τ from the numerical computations and the results obtained from the analytic expression according to Eq. (13).

$\tau(\beta) = \Gamma_0 + \Gamma_1\beta + \Gamma_2\beta^2$, which corresponds to a quadratic polynomial as shown in Fig. 5. In Fig. 10 we compare the value of the parameter τ obtained from the numerical computations and the results of the analytic formula of Eq. (13).

Now we obtain a reasoning for the parameter α as a function of β according to Eq. (6) in the open nonhyperbolic regime. Toward this goal, we consider the stickiness effect of the KAM islands in the trajectories which leave the scattering region and eventually pass through the KAM tori. The basic idea is well explained in [22]. If a process that decays (or grows) exponentially is killed randomly, then the distribution of the killed state will follow a power law in one or both tails. Indeed, we can consider that all the particles leaving the scattering region follow an exponential decay law, but because some of the trajectories pass close to the KAM islands, the exponential decay process is killed during a certain time. The average result is that the decay law when sizable KAM tori exist is algebraic. Therefore, if we consider the exponential decay law of the particles $P(t) = e^{-\tau t}$ killed at a random time T which is exponentially distributed with parameter ν , then the killed state $\bar{P} = e^{-\tau T}$ has the probability density function $f_{\bar{P}}(t) = (\frac{\nu}{t})t^{-\frac{\nu}{t}}$ for $t > 1$. Therefore, the average decay law of the particles shows a power-law behavior. For the sake of clarity, τ is the parameter of Eqs. (12) and (13), which regulates the exponential decay law of the particles. When a particle trajectory passes close to a KAM island, the KAM stickiness causes that the escape process is killed during a certain time. Indeed as shown in Fig. 3, the higher the energy of the system is, the smaller the area of the KAM island is. Therefore, we can consider that for higher energies it is more difficult for a certain trajectory to pass close to KAM islands. The exponential decay of the particles is more likely to be killed at low energies than at higher energies. In that sense the parameter ν is directly related to the energy of the system so we can rewrite the expression for $f_{\bar{P}}(t)$ as a function of β as $f_{\bar{P}}(t) = (\frac{g(\beta)}{t})t^{-\frac{g(\beta)}{t}}$. The function which relates ν to β is $g(\beta)$. Comparing $f_{\bar{P}}(t)$ with Eq. (6), we can write $\alpha(\beta) = \frac{g(\beta)}{1-\tau(\beta)}$.

We have proposed an expression for $g(\beta)$ that matches quite well the numerical values obtained for $\alpha(\beta)$ as

$$g(\beta) = \frac{1}{D_{PS}\sqrt{\Phi_{KAM}}},$$

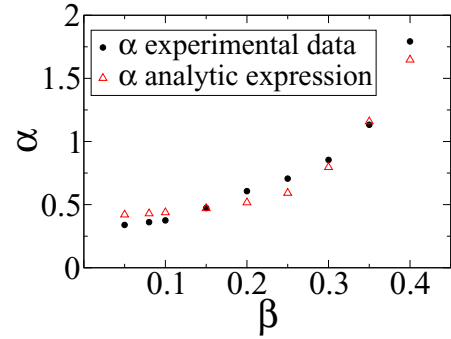


FIG. 11. Comparison between the data for parameter α from the numerical computations and the results obtained from the analytic expression according to Eq. (14).

where D_{PS} is the dimension of the phase space of the system, in this case, $D_{PS} = 4$. According to the proposed expression, $g(\beta)$ is inversely proportional to the area of the KAM island due to the term $\frac{1}{\sqrt{\Phi_{KAM}}}$ and also to the dimension of the phase space. The higher the dimension of the phase space is, the less probable it is that a particle will reach the KAM region since there are other directions in which it can go. The obtained formula to express the parameter α as a function of β is

$$\alpha(\beta) = \frac{1}{D_{PS} \frac{1}{\sqrt{\Phi_{KAM}}}} \frac{1}{1-\tau(\beta)}. \quad (14)$$

In Fig. 11 we compare the value of the parameter α obtained from the numerical computations and the results from the analytic formula of Eq. (14).

We have seen throughout this work that the dynamics of the relativistic Hénon-Heiles mainly depends on the evolution of the topology of the phase space when we vary β . In particular, we have concluded that the existence of KAM islands in the phase space of the system is the key driver to exhibit a nonhyperbolic or a hyperbolic dynamics, regardless of the value of β . From this point of view, the global properties of the system which depend on the topology of the phase space may vary even for low velocities. Although the Hénon-Heiles potential was initially developed to model the motion of stars around an axisymmetrical galaxy, we think that the phenomena described in the present work may be related to many other real phenomena that occur in Nature. For instance, the M -sigma relation is an empirical correlation between the stellar velocity dispersion σ of a galaxy bulge and the mass M of the supermassive black hole at its center (see Refs. [23] and [24]). This correlation is quite relevant since it is commonly used to estimate black-hole masses in distant galaxies using the easily measured quantity σ . The M -sigma relation is well described by an algebraic power law, and although the applications of the Hénon-Heiles and the M -sigma models are very different, we speculate that the underlying mathematical properties are similar, including the presence of KAM islands in the phase space of both systems. Therefore, the KAM islands would be responsible for the algebraic decay law, and hypothetically, their destruction would imply an exponential decay law to relate σ to the mass M of a supermassive black hole.

VII. CONCLUSIONS

In the last years, there has been important progress in understanding the relativistic effects in chaotic scattering. Most research has focused on studying the discrepancies between the Newtonian and the relativistic approaches over the trajectories of the particles (see Refs. [6–9]). More recently, there have been some results on the dimension of the nonattracting chaotic invariant set of a chaotic scattering system based on the four-hill potential (see Ref. [10]). They state that this global property of the system can be accurately predicted by the Newtonian approximation in slow chaotic scattering motion. Here we show that some other relevant global properties of chaotic scattering systems do depend on the effect of the Lorentz transformations and we may consider the relativistic corrections when we want to describe them in a realistic manner, even for low velocities. We have used the Hénon-Heiles system as a model reference for the theoretical reasoning and for the numerical computations.

We consider that the global properties of the Hénon-Heiles system vary because the Lorentz corrections destabilize the topology of the phase space. In this sense, according to the regime of energies we have chosen for our numerical calculations, the KAM islands are fully destroyed for $\beta \approx 0.4$. We have proved in Fig. 2 that the average escape time \bar{T}_e in the Hénon-Heiles system decreases when β increases. Indeed at $\beta \approx 0.4$ there is a leap where the linear trend of \bar{T}_e changes

abruptly. This can be easily explained from the perspective of KAM island destruction (see Fig. 3). We have explained the shape of the curves $\bar{T}_e(\beta)$, $\alpha(\beta)$, and $\tau(\beta)$ in Figs. 2, 4, and 5 by energetic considerations. We have also characterized the decay laws of the open nonhyperbolic and hyperbolic regimes, obtaining algebraic expressions that fit the data from our numerical computations.

Finally, we have speculated about the possibility of finding this dependence of the global properties of the system on the topology of the phase space in many other phenomena in Nature. For instance, the M - σ correlation (see Refs. [23] and [24]) is well described by an algebraic power law. We may consider that this relation is due to the presence of KAM islands in the phase space. Its destruction would involve an exponential decay law.

ACKNOWLEDGMENTS

This work was supported by the Spanish Ministry of Economy and Competitiveness under Project No. FIS2013-40653-P and by the Spanish State Research Agency (AEI) and the European Regional Development Fund (FEDER) under Project No. FIS2016-76883-P. M.A.F.S. acknowledges the jointly sponsored financial support by the Fulbright Program and the Spanish Ministry of Education (Program No. FMECD-ST-2016).

-
- [1] J. M. Seoane and M. A. F. Sanjuán, *Rep. Prog. Phys.* **76**, 016001 (2012).
 - [2] E. Ott and T. Tél, *Chaos* **3**, 417 (1993).
 - [3] C. Grebogi, E. Ott, and J. A. Yorke, *Physica D* **7**, 181 (1983).
 - [4] T. Tél and B.-L. Hao, *Directions in Chaos*, Vol. 3, edited by B.-L. Hao (World Scientific, Singapore, 1990), p. 149; T. Tél and B.-L. Hao, in *STATPHYS 19*, edited by B.-L. Hao (World Scientific, Singapore, 1996), p. 243.
 - [5] H. C. Ohanian, *Special Relativity: A Modern Introduction* (Physics Curriculum & Instruction, Lakeville, MN, 2001).
 - [6] B. L. Lan, *Chaos* **16**, 033107 (2006).
 - [7] B. L. Lan, *Chaos Solitons Fractals* **42**, 534 (2009).
 - [8] B. L. Lan and F. Borondo, *Phys. Rev. E* **83**, 036201 (2011).
 - [9] S.-N. Liang, B. L. Lang, *Results Phys.* **4**, 187 (2014).
 - [10] J. M. Aguirregabiria, [arXiv:1004.4064v1](https://arxiv.org/abs/1004.4064v1).
 - [11] J. D. Bernal, J. M. Seoane, and M. A. F. Sanjuán, *Phys. Rev. E* **88**, 032914 (2013).
 - [12] M. Hénon and C. Heiles, *Astron. J.* **69**, 73 (1964).
 - [13] R. Barrio, F. Blesa, and S. Serrano, *Europhys. Lett.* **82**, 10003 (2008).
 - [14] G. Contopoulos, *Astron. Astrophys.* **231**, 41 (1990).
 - [15] J. M. Seoane and M. A. F. Sanjuán, *Phys. Lett. A* **372**, 110 (2008).
 - [16] J. M. Seoane, L. Huang, M. A. F. Sanjuán, and Y.-C. Lai, *Phys. Rev. E* **79**, 047202 (2009).
 - [17] J. M. Seoane and M. A. F. Sanjuán, *Int. J. Bifurcat. Chaos* **20**, 2783 (2010).
 - [18] C. F. F. Karney, *Physica D* **8**, 360 (1983); B. V. Chirikov and D. L. Shepelyansky, *ibid.* **13**, 395 (1984); J. Meiss and E. Ott, *ibid.* **20**, 387 (1986); Y.-C. Lai, M. Ding, C. Grebogi, and R. Blümel, *Phys. Rev. A* **46**, 4661 (1992).
 - [19] M. Ding, T. Bountis, and E. Ott, *Phys. Lett. A* **8**, 395 (1991).
 - [20] H. J. Zhao and M. L. Du, *Phys. Rev. E* **76**, 027201 (2007).
 - [21] M. C. Gutzwiller, *Chaos in Classical and Quantum Mechanics* (Springer, New York, 1990).
 - [22] W. J. Reed and B. D. Hughes, *Phys. Rev. E* **66**, 067103 (2002).
 - [23] F. Ferrarese and D. Merritt, *Astrophys. J.* **539**, L9 (2000).
 - [24] K. Gebhardt, R. Bender, G. Bower, A. Dressler, S. M. Faber, A. V. Filippenko, R. Green, C. Grillmair, L. C. Ho, J. Kormendy, T. R. Lauer, J. Magorrian, J. Pinkney, D. Richstone, and S. Tremaine, *Astrophys. J.* **539**, L13 (2000).